Published in final edited form as:
Alcohol. 2012 November ; 46(7): 619–627. doi:10.1016/j.alcohol.2012.07.003.

Ethanol-induced disruption of Golgi apparatus morphology, primary neurite number and cellular orientation in developing cortical neurons

Teresa A. Powrozek[1,2] and **Eric C. Olson**[1,2]

[1]Department of Neuroscience and Physiology, SUNY Upstate Medical University, Syracuse, NY 13210

[2]Developmental Exposure Alcohol Research Center, SUNY Binghamton University, Binghamton, NY 13902

Abstract

Prenatal ethanol exposure disrupts cortical neurite initiation and outgrowth, but prior studies have reported both ethanol-dependent growth promotion and inhibition. To resolve this ambiguity and better approximate *in vivo* conditions, we quantitatively analyzed neuronal morphology using a new, whole hemisphere explant model. In this model, Layer 6 (L6) cortical neurons migrate, laminate and extend neurites in an organotypic fashion. To selectively label L6 neurons we performed *ex utero* electroporation of a GFP expression construct at embryonic day 13 and allowed the explants to develop for 2 days *in vitro*. Explants were exposed to (400mg/dL) ethanol for either 4 or 24 hrs prior to fixation. Complete 3-D reconstructions were made of >80 GFP-positive neurons in each experimental condition. Acute responses to ethanol exposure included compaction of the Golgi apparatus accompanied by elaboration of supernumerary primary apical neurites, as well as a modest (~15%) increase in higher order apical neurite length. With longer exposure time, ethanol exposure leads to a consistent, significant disorientation of the cell (cell body, primary apical neurite, and Golgi) with respect to the pial surface. The effects on cellular orientation were accompanied by decreased expression of cytoskeletal elements, microtubule associated protein 2 and F-actin. These findings indicate that upon exposure to ethanol, developing L6 neurons manifest disruptions in Golgi apparatus and cytoskeletal elements which may in turn trigger selective and significant perturbations to primary neurite formation and neuronal polarity.

Keywords

preplate splitting; Golgi apparatus; Fetal Alcohol Syndrome

To whom correspondence should be addressed: Eric C. Olson, PhD, Department of Neuroscience and Physiology, SUNY Upstate Medical University, 3295 Weiskotten Hall, 750 E. Adams St. Syracuse, NY 13210, olsone@upstate.edu, Phone: 315-464-7776, FAX: 315-464-7712.

Competing Interests
The authors declare that they have no competing interests.

Author's Contributions
EO and TP designed the study. TP performed the study and TP and EO co-authored the manuscript.

INTRODUCTION

Prenatal exposure to ethanol is a leading cause of mental retardation (Jones and Smith, 1973) with the developing cerebral cortex particularly vulnerable to ethanol exposure. Studies conducted primarily in rodent have reported ethanol-induced impairments in neurogenesis (Goodlett and Horn, 2001), neuronal migration (Aronne et al., 2011) and axonal outgrowth (Granato et al., 2003; Lindsley et al., 2003; Livy and Elberger, 2008). Regarding the latter, low (12.5 mM) concentrations of ethanol impair growth cone responses to guidance cues, including semaphorins and netrins (Sepulveda et al., 2011), known to regulate axonal growth and targeting (Behar et al., 1996; Luo et al., 1995; Serafini et al., 1994; Steup et al., 2000). Attention has also been directed to ethanol-mediated suppression or enhancement of dendritic growth (Granato and Van Pelt, 2003; Lawrence et al., 2012; Yanni et al., 2002). The consequences of ethanol exposure upon dendritogenesis appear to be context specific, and may depend on the presence or absence of astrocyte-derived factors. Ethanol dependent changes in spine density may also compound the disruption of dendritic structure (Hamilton et al., 2010; Whitcher and Klintsova, 2008) and depend on cortical area and cell class. The combination of ethanol effects may contribute to altered excitability of the dendritic arbor (Granato et al., 2012).

Although much cortical dendritic growth occurs postnatally, recent studies have demonstrated that dendritic initiation occurs prenatally, coincident with neuronal migration arrest and cellular positioning (Nichols and Olson, 2010; Olson et al., 2006). Early cortical development may therefore represent a critical period for ethanol-induced teratogenesis; particularly in regards to dendritic initiation, growth, and function.

To explore and characterize potential negative consequence(s) of ethanol exposure upon apical neurite initiation and growth, and to gain insights into possible mechanisms underlying cytoarchitectural effects of ethanol exposure, we exposed cortical explants to ethanol during an early period of cortical development that includes Layer 6 (L6) neuron dendritogenesis. A new, whole cerebral hemisphere explant model was used, in which prospective L6 neurons develop in an organotypic fashion during the period of neuronal positioning and dendritic initiation (Nichols and Olson, 2010; O'Dell et al., 2012). This explant system permits precise control of ethanol delivery and dosage while preserving all cell-cell and cell-extracellular matrix interactions that are likely required for proper neuronal growth and differentiation. Using this approach, we report significant disruptions in cortical neuron development, particularly at the level of apical neurite growth. We observed a rapid increase in primary apical neurite number accompanied by condensed Golgi morphology after 4 hrs of ethanol exposure. Cumulative exposure for 24 hrs leads to significant disorientation of neurites and cell bodies accompanied by altered content of the essential cytoskeletal elements F-actin and microtubule associated protein 2 (MAP2).

METHODS

Mice

The Institutional Animal Care and Use Committee of SUNY Upstate Medical University approved all animal procedures. Time pregnant Swiss Webster mice (Taconic Laboratories, Germantown, NY) were obtained at embryonic day 12 (E12). The day of plug discovery was designated embryonic day 0 (E0).

Ex Utero Electroporation

Pregnant dams were sacrificed by CO_2 inhalation on E13. Embryos were removed from the uterus *via* caesarean section and submerged in cold Hanks Balanced Saline Solution (HBSS, Invitrogen Life Technologies, Grand Island, NY). *Ex utero* electroporations were then

performed on intact embryos. A plasmid encoding the chicken actin globin (CAG) promoter coupled to an enhanced Green Fluorescence Protein coding sequence (CAG-eGFP) (Matsuda and Cepko, 2004) was prepared at a concentration of 0.33 mg/ml with 0.01% Fast Green dye in sterile water. Using a Hamilton syringe fitted with a #30 beveled needle, 2–3 μl of plasmid DNA solution was injected so as to fill the lateral ventricle completely. Successful injections were ascertained by the filling of the lateral ventricle with Fast Green dye. Tweezer electrodes connected to a BTX830 electroporator (Harvard Apparatus, Holliston, MA) were then positioned on the head of the embryo with the anode positioned along the cerebral midline and the cathode under the chin. DNA was electroporated with five 30 V pulses of 50 msec duration with an interpulse interval of 950 msec. This recently developed *ex utero* electroporation approach (O'Dell et al., 2012) allowed consistent targeting of the dorsomedial region of the neocortex (Embryonic Field 1) (Takahashi et al., 1995). After electroporation, the embryos were kept in ice-cold HBSS until dissection and whole hemisphere explant preparation (below). The interval between electroporation and dissection did not exceed 1 hr.

Cortical Explant Cultures

A whole hemisphere explant model was utilized in which organotypic development is observed for a period of 2 days *in vitro* (DIV) (Nichols and Olson, 2010; O'Dell et al., 2012). Following electroporation, the whole brain was removed from the embryo and divided along the sagittal midline. The left (electroporated) hemisphere was further dissected from hindbrain and cerebellar anlage, taking care to leave sub-cortical matter and the meninges intact. The hemispheres were then placed midline down, onto a collagen-coated, polytetrafluoroethylene (PTFE) filter with a 3-μm pore size (TranswellCOL, Corning). The filters were then placed in 2.7 ml DMEM-F12 media containing Glutamax and supplemented with 2% B-27, 1% G5 and 1% Penicillin- Streptomyocin (Invitrogen Life Technologies, Grand Island, NY). Explants were then placed in a high oxygen (95% O_2/5% CO_2) incubator chamber (Billups-Rothenberg, Del Mar, CA) at 37°C. At either 24 or 4 hrs prior to fixation culture media was brought to 87 mM ethanol (400 mg/dl) or treated with equivalent volumes (13.7μl) of sterile H_20 (Control). The elapsed time between electroporation and placing the cultures in the incubator never exceeded 1.5 hrs.

Histology

Following 48 hrs of total culture time, the explants were fixed in 4% paraformaldehyde in Pagano buffer (250 mM sucrose, 25 mM $MgCl_2$, 2.5 mM KCl, 50mM HEPES; pH = 7.4) for one hr. The hemispheres were then embedded in 10% gelatin blocks, post-fixed for 24 hrs in 4% paraformaldehdye/Pagano solution and sectioned at 100 μm thickness using a Vibratome (Ted Pella, Redding, CA). For immunohistochemical processing the sections were first incubated in phosphate buffered saline containing 0.5% Triton-X 100 and 2% bovine serum albumin (PBST+B) pH 7.4 for one hr prior to overnight incubation in primary antibody (diluted in PBST+B). The sections were washed 3 times in PBS and then incubated in appropriate secondary antibodies (diluted in PBST+B) for 2 hrs. The primary antibodies were anti-GM130 (1:150, BD Biosciences, San Jose, CA) and anti-microtubule associated protein 2 (MAP2; 1:1000, Sigma, St. Louis, MO). The secondary antibodies were AlexaFluor-conjugated anti-mouse and anti-rabbit (1:500, Invitrogen Life Technologies, Grand Island, NY) used at a 1:500 dilution. AlexaFluor 555-conjugated Phalloidin (1:200, Invitrogen Life Technologies, Grand Island, NY was used to detect F-actin. Hoechst 33342 (2 μg/mL, Invitrogen Life Technologies, Grand Island, NY) was used for visualization of individual cell nuclei.

SDS-PAGE and Western Blot Analysis

Whole cerebral hemisphere lystates were prepared in cold RIPA lysis buffer (20 mM Tris, pH 7.5, 150 mM NaCl, 1.0% Nonidet P-40, 0.50% sodium deoxycholate, 1.0 mM EDTA, and 0.10% SDS supplemented with a protease inhibitor cocktail (P-8340, Sigma, St. Louis, MO), 1.0 mM sodium orthovanadate, and 20 mM sodium fluoride. The samples were homogenized and centrifuged for 10 min at 15,300 × g. Protein samples (30 μg) were combined with sample buffer (300 mM Tris-HCl, 50% glycerol, 5.0% SDS, 0.025% bromophenol blue, and 250 mM β-mercaptoethanol) and separated by SDS-PAGE using a 4–15% TGX gradient gel, (Bio-rad, Hercules, CA). The separated proteins were transferred to Immobilon-P (polyvinlyidene difluoride) membranes (EMD Millipore, Billerica, MA) for subsequent immunoblotting.

The immunoblotting followed a three-step procedure. Nonspecific immunoreactivity was blocked in Tris buffered saline containing 0.01% Tween-20 and 3% bovine serum albumin (TBST+B) for 1 hr at room temperature. The membranes were then incubated overnight with a primary antibodies diluted in TBST+B. The primary antibodies were anti-MAP2 (1:1000, clone HM-2, Sigma, St. Louis, MO), anti-Tbr1 (1:1000, Abcam, Cambridge, MA) and anti-GM130 (1:500, BD Biosciences, San Jose, CA). Membranes were rinsed 3X in TBST and incubated with either a horseradish peroxidase (HRP)-linked anti-mouse or anti-rabbit secondary antibody (1,10:000; Bio-Rad, Hercules, CA). HRP activity was visualized using chemiluminescence (Supersignal WestPico, Thermo Fisher Scientific, Waltham, MA) detected by Kodak Biomax XAR film. To ensure equal protein loading in each lane, membranes were then stripped in a buffer containing 62.5 mM Tris-HCl, 2.0% SDS, and 10 μM β-mercaptoethanol at 50°C for 30 min and reprobed with the anti-Tbr1 antibody.

Imaging and analysis

Images were collected with a Zeiss LSM510 laser scanning confocal microscope (SUNY Upstate Medical University Center for Bioresearch Imaging). Digital images (z-stacks) were collected at 1 μm z-step interval typically through 60 μm of tissue. The stacks were then imported into FIJI (www.fiji.sc), an open source distribution of Image J (Wayne Rasband, NIH). To determine apical neurite lengths and branching, one z-stack was analyzed per explant. A maximum of 6 cells were traced in each z-stack for an average of 80 cells analyzed *per* treatment group. The cells were selected by an investigator blinded to treatment status. Within each z-stack, cells for analysis were selected along the lateral to dorsal transneural genetic gradient (Takahashi et al., 1995) (Supplemental Figure 1A) to ensure that there was no bias in neuronal maturity of the selected cells. Only neurons within 50 μm of the pial surface were analyzed as these were previously shown to be Tbr1 and Ctip2 positive (L6 neuronal markers, O'Dell et al, 2012). 3-D reconstructions (Figure 1A) were made using the open source Simple Neurite Tracer plugin in the FIJI package (Longair et al., 2011). The axon was readily recognized as the fine caliber neurite extending from the base (ventricular side) of the soma (Figure 1C and Supplemental Figure 1A) and was excluded from analysis. Tracing was then only performed on those cells that had all their remaining neurites contained within the image stack. Cells were excluded if located within ~100 μm of a heterotopia. Although leptomeningeal heterotopias can be caused by ethanol (Komatsu et al., 2001), and were occasionally observed in our 24 hr-treated explants, neurons in these areas were avoided for the purpose of analysis as any abnormal cellular morphology might then be a result of the changes in the cellular environment due to the hetereotopia, rather than a direct effect of ethanol on cellular morphology. The apical neurite length and branching values were determined within FIJI and exported to Excel. The quantified apical arbor was divided into two categories for analyses: namely, primary apical neurites (neurites emitted directly from the neuronal soma) and higher order apical neurites (all non-primary apical neurites). This approach was adopted because primary neurites are

thought to directly reflect neuronal polarity (Horton et al., 2005; Matsuki et al., 2010; Nichols and Olson, 2010) and may differentially respond to ethanol exposure.

Orientation Measures

A custom MATLAB (Version 7.14, Mathworks Inc. Natick, MA) script was developed to determine orientation angle of the primary neurite and cell soma with respect to the shortest path tangent to the pial surface. First, the pial surface was manually traced in each z-step of the stack; these contour lines were imported into MATLAB and interpolated as a surface. The skeletonized neuron (Figure 1B) from Simple Neurite Tracer was imported and the shortest distance between the rendered neuronal soma and the interpolated surface was determined. The angles between the shortest line to the surface and either the primary neurite or the long axis of the neuronal soma were then determined in 3-D (Figure 1C).

Golgi Elongation Measurement

Proximal to distal Golgi length measurements were made of Golgi localized within GFP+ cells by tracking the GM130 immunosignal through the z-series that contained the cell. Orientation of the Golgi was determined from the angle subtended between proximal/distal line and the shortest path to the overlying pia. The angle was then assigned to a quadrant (Q1–Q4, each occupying 90° around the cell soma). Quadrants 2 and 3 were combined in the analysis, as these left/right orientation angles depended upon the arbitrary orientation of the mounted section. Five cells were quantified per explant, and averaged. These per-explant averages were then compared between treatments groups.

Immunofluorescence Signal Analysis

Control and experimental brain sections were processed in parallel. Images were acquired at the same z-depth and in similar locations in the dorsal cortex with matched acquisition parameters (laser power, gain, blacklevel, pinhole size and zoom). Image quantification was achieved in ImageJ by placing ROIs (Regions of Interest) within the marginal zone (MZ) that is enriched in L6 dendrites (Nichols and Olson, 2010), the cortical plate (CP) that contains the L6 neuron cell bodies (O'Dell et al., 2012) and the intermediate zone (IZ) that contains immature multipolar cortical neurons and L6 axonal processes (Hatanaka and Yamauchi, 2012; Tabata and Nakajima, 2003). Following background correction, the mean pixel value of each ROI was measured and the measurements were exported to Excel for further comparison.

Statistical Analysis

Differences among the treatment groups were analyzed using a one-way ANOVA across treatment times (0, 4 and 24 hrs). In cases where data was binned (e.g., Golgi orientation), a one-way mixed measures ANOVA across treatment time and ROI, was run. Upon detection of significance, Fishers LSD was used for post-hoc analysis. In some cases the data failed the Shapiro-Wilk normality test and thus a Kruskal-Wallis One Way ANOVA on Ranks was performed. Significant differences ($p < 0.05$) were then ascertained by post-hoc Dunn's pair wise comparison.

RESULTS

Ex utero electroporation labeling of Layer 6 neurons

To label L6 neurons for subsequent morphological characterization, we performed *ex utero* electroporations of a GFP expression construct (CAG-eGFP) on E13 mouse embryos. Immediately after electroporation, whole hemisphere explants were prepared and cultured for 48 hrs. A single dose ethanol exposure was performed during hours 24–48 (24 hr dose)

or hours 44–48 (4 hr dose) immediately prior to fixation and histology. During the explant culture period (E13–E15) GFP labeled prospective L6 neurons migrate from the ventricular zone (VZ) through the IZ, where they initiate axonal development (Hatanaka and Yamauchi, 2012), and position themselves in the forming cortical plate (CP) where they initiate dendritic development. The GFP+ neurons found within the CP at 48 hrs post electroporation express the transcription factors Ctip2 and Tbr1 that identify L6 cortical neurons during this time in cortical development (O'Dell et al., 2012). Two exposure times were chosen to distinguish the acute (4 hr) ethanol responses of cells within the area of analysis (i.e., within 50 μm of the pial surface, see Methods), from the cumulative (24 hr) response that would represent neurons exposed for 24 hrs within the area of analysis and also be expected to include a population of cells that migrated into the area of analysis during the exposure period. The appropriate transcription factor expression and normal migration behavior of these GFP+ neurons as well as the growth of CP in the portion of the explant corresponding to dorsomedial cortex verify organotypic cortical development is occurring during the culture period (Nichols and Olson, 2010).

Dendritic outgrowth and arborization

To quantify the morphology of L6 neurons after 4 and 24 hrs of ethanol exposure, confocal z-series were acquired through 60 μm of tissue and complete 3-D rendering of the GFP+ neurons in the CP were then generated (Supplemental Movies 1, 2 and 3). The neurites of neurons contained in these 3-D reconstructions were then traced using Simple Neurite Tracer (Longair et al., 2011) for subsequent quantification of neurite morphology. A set of representative flattened images (Figure 2A–C) and traced neurons (Figure 2D) illustrate the morphological changes seen following ethanol exposure. While neurites continue to elaborate in ethanol treated explants, the cells appear to have abnormal orientations of both their cell body and neurites. In contrast to the pial directed growth of control neurites, a number of the neurites of ethanol treated cells appeared to grow away from the pial surface (red arrows).

The complete 3-D neurite tracings were then analyzed to obtain the apical neurite lengths and branching patterns of control and ethanol treated neurons. For these analyses, neurites extending directly from the cell body are referred to as "primary apical neurites" and these primary apical neurites were analyzed as a separate category from the remaining apical neurites which are called "higher order apical neurites" (Figure 3). Both 4 and 24 hrs of ethanol exposure modestly increased higher order apical neurite length (~ 15%) compared to control (Figure 3A; $p < 0.01$), but did not change the total number of higher order apical neurites (Figure 3C; $p = 0.59$). Although ethanol exposure did not affect the total number of higher order neurites, the organization of the arbor did change. The number of primary apical neurites (neurites extending directly from the neuronal soma, Figure 3B) increased in response to ethanol exposure: 27% of control neurons extend more than one primary apical neurite (1.30 ± 0.06), whereas 56% of ethanol treated neurons exhibited multiple primary apical neurites (2.07 ± 0.12), with some ethanol treated neurons extending up to eight primary apical neurites (Figure 3C, D). This effect was seen following 4 hrs of ethanol exposures, indicating a rapid reorganization of the dendritic arbor in response to ethanol.

As a consequence of the radial organization of the cerebral cortex, most cortical excitatory neurons orient their apical neurite and cell soma towards the pial surface. To measure the orientation of the neurite and soma, the skeletonized neuron from Simple Neurite Tracer along with the traced pial surface was imported into MATLAB. A custom script then determined the shortest path extending from the neuronal soma to the pial surface. The angle of the primary apical neurite and the long axis of the neuronal soma made with respect to that shortest line was then determined (Figure 1; See Methods). The primary apical neurite of control neurons extends at an angle of 46 ± 2.4° with respect to the shortest path to pia

while neurons exposed to ethanol for 24 hrs displayed a significantly different neurite orientation (60 ± 3.7°) (Figure 4B). Similar values and effects were observed for somal orientation with respect to the pial surface (Figure 4A). Taken together these observations indicate that acute ethanol exposure triggered a rapid (<4 hrs) formation of supernumerary primary apical neurites and modest increase in apical neurite length. Cumulative ethanol exposure for 24 hrs caused a change of the soma and primary apical neurite orientation.

Golgi Elongation and F-actin Expression

For most excitatory cortical neurons the axon emerges as the migrating neuron moves through the IZ. At this time the position of the Golgi apparatus and the centrosome anticipates the site of axon emergence (de Anda et al., 2010). During subsequent dendrite initiation in the CP, the Golgi apparatus shifts to the opposite side of the developing pyramidal neuron and becomes invested in the apical dendrite, forming Golgi “outposts” that are required for asymmetric dendritic growth (Horton et al., 2005; Matsuki et al., 2010; Nichols and Olson, 2010). To assess whether ethanol exposure causes abnormalities of Golgi positioning or investment in the apical neurite, we immunostained treated neurons for the cis-Golgi marker GM130 (Nakamura et al., 1995). Whereas neurons in control explants had clearly elongated Golgi structures within the GFP+ neurons that could extend into the primary apical process (Figure 5A), both 4 and 24 hr ethanol exposure (Figure 5B, C) resulted in apparent compaction of the Golgi, creating a more “ball-like” structure manifest in a 41% reduction in the organelle’s proximal-to-distal length ($p < 0.001$; Figure 5D). This ethanol-dependent compaction of the Golgi was accompanied at 24 hrs by an intracellular repositioning, such that the Golgi was more likely to occupy lateral areas of the neuronal soma (Figure 5E). This change in GM130 immunostaining does not seem to correspond to a loss of GM130 protein in whole explant lysates (Figure 5F). Thus both cumulative (24 hr) and acute (4 hr) ethanol exposure causes Golgi apparatus compaction, while Golgi redistribution was only observed with cumulative exposure.

The Golgi apparatus is believed necessary for forward secretory trafficking of cytoskeletal proteins and plasma membrane components necessary for normal dendritic growth (Ye et al., 2007). We therefore screened for possible effects of ethanol exposure upon two indicators of cytoskeletal architecture, F-actin and MAP2. To perform this analysis, ROIs were placed to measure average signal intensity within the MZ, CP and IZ (Figure 6A; **top row**). Both 4 hr (Figure 6B, D, $p < 0.001$) and 24 hr (Figure 6C, D, $p < 0.001$) ethanol exposure caused a significant reduction in F-actin content, which was particularly pronounced at the MZ (Figure 6D). Similarly, the levels of MAP2 immunofluorescence were significantly ($p < 0.05$) reduced in the MZ of ethanol treated explants, but only after 24 hr exposure ($p < 0.01$) to ethanol (Figure 6E). The reduction of immunofluorescence was confirmed by Western blot analysis of whole hemisphere lysates (Figure 6F). A reduction in level of mature MAP2 (the a and b isoforms) was observed by 24 hrs, with little change apparent at 4 hrs. In contrast, the “immature” form of MAP2 (c isoform) showed little change at 4 and 24 hrs. Thus, coincident with disruptions of neuronal orientation and apical neurite growth, we observe disruption(s) to the Golgi apparatus and cytoskeletal components known to be critical for neurite growth and stability.

DISCUSSION

Our investigations revealed acute (4 hr) and cumulative (24 hr) responses of developing L6 neurons to ethanol exposure within an organotypic environment. The acute responses are characterized by Golgi apparatus compaction and an increase in the number of primary apical neurites. Higher order apical neurite length, however, is only slightly increased. The cumulative responses are characterized by both persistence of the more acute effects, as well

as diminished MAP2 and F-actin content in the MZ, and a significant disorientation of the neuron with respect to the pial surface.

Although the neurites of these very immature cells were not strongly immunopositive for the canonical dendritic marker MAP2, or the canonical axonal marker SMI312 (Supplemental Figure 1A, B), it is well established that immature postmitotic neurons *in vivo* and *in vitro* have multiple neurites, one of which is specified as the axon while the remaining neurites become specified as dendrites (Dotti and Banker, 1987; Dotti et al., 1988; Hatanaka and Yamauchi, 2012; Tabata and Nakajima, 2003). For maturing cortical neurons axon specification occurs during migration through the intermediate zone (Hatanaka and Yamauchi, 2012). The remaining neurites become dendrites once the migrating neuron has reached the top of the CP (O'Dell et al., 2012; Olson et al., 2006). Since all of the neurons analyzed were 1) in the forming CP and 2) showed a fine caliber axon that descended towards the forming white matter/IZ, it is likely that the apical neurites analyzed in this study are nascent dendrites.

The centrality of the Golgi apparatus to the developing dendrite has been identified and highlighted in several recent publications (Horton et al., 2005; Matsuki et al., 2010; Nichols and Olson, 2010; Ye et al., 2007). In the emerging model, appropriate deployment of the Golgi apparatus is required for both proper orientation and growth of the dendritic arbor. Dendritic orientation is thought to emerge from the coupling of cellular polarity mechanisms including Reelin/Dab1 signaling, operating in opposition to LKB1/Stradα signaling, to localize the Golgi at the appropriate site for dendritic initiation and growth (Matsuki et al., 2010; Shelly et al., 2011; Shelly and Poo, 2011). The Golgi then could provide a number of functions supportive to the emerging dendrite, including acting as a microtubule nucleating center (Kodani and Sutterlin, 2009) and providing the cellular membrane and proteins required for process extension and growth (Horton et al., 2005; Ye et al., 2007).

Several functions of the Golgi apparatus are known to be sensitive to ethanol exposure; ethanol inhibits glycoprotein trafficking and causes impairment of exocytosis and endocytosis (Marin et al., 2010; Megias et al., 2000; Tomas et al., 2002; Tomas et al., 2005). Impairment of these essential cellular functions could alter the adhesive (Greenberg, 2003) or chemotropic properties (Sepulveda et al., 2011) of the neurite and produce the observed alterations in neuronal cytoskeletal structure and morphology, including the reduction of polymerized tubulin and actin assembly within the extending dendrite (Romero et al., 2010).

Function of the Golgi apparatus may also be sensitive to metabolites of ethanol including acetaldehyde (Marinari et al., 1993). Acetaldehyde is a teratogen in its own right that can potentiate the negative consequences of ethanol consumption during pregnancy (Chen et al., 1995; Qu and Wu, 1999). While the fetal brain does metabolize ethanol into acetaldehyde via catalase (Hamby-Mason et al., 1997), the *in vivo* environment would contain acetaldehyde metabolized by both mother and fetus. Thus ethanol exposure might be more disruptive of Golgi function *in vivo* than in the whole hemisphere explant model.

Ethanol might also disrupt cellular polarity by delocalizing the Golgi apparatus from the apical (pial) side of the neuron (Figure 5E). Prior studies have suggested a direct relationship between Golgi localization and polarized dendritic growth in the cortex and hippocampus (Matsuki et al., 2010; Nichols and Olson, 2010). Similarly, Golgi position anticipates the developing Purkinje neuron primary dendrite and blockade of atypical PKC (aPKC) function disrupts Golgi position and causes cells to display multiple primary dendrites (Tanabe et al., 2010). Thus the compaction and de-localization of the Golgi from the primary apical dendrite observed in this study may contribute both to the increase in primary dendrite number and the loss of F-actin and MAP2 content in the dendritic processes.

Ethanol exposure is also known to alter the neuronal expression of critical cytoskeletal regulatory genes. The expression of RhoA, Paxillin, CDC42 and DYNLL1 are rapidly induced following exposure to a single dose of ethanol in fetal cerebral cortical cell cultures (Camarillo and Miranda, 2008). Interestingly, DYNLL1, a subunit of the minus-end microtubule motor complex Dynein, is responsible for directing Golgi outposts into dendrites, enabling their branching and growth (Marin et al., 2010; Ye et al., 2007). Ethanol may thus interfere with neuronal polarity and dendritic growth through multiple, possibly interacting, mechanisms at the level of the cytoskeleton and Golgi apparatus.

The ethanol-dependent disruptions of L6 neurons identified in this study may manifest functional consequences that persist into postnatal life. While the whole hemisphere explants show organotypic growth for 2–3 DIV, this period does not encompass the synaptogenic period for L6 neurons. Thus the electrophysiological consequences of ethanol exposure cannot be directly assessed in the whole hemisphere explant model. However, L6 neurons are the first neurons to populate the forming CP and do so by splitting the preplate into the MZ and subplate (Marin-Padilla, 1978). Failure to correctly split the preplate is associated with later cortical disruptions including aberrant thalamocortical axonal pathfinding and disrupted cortical migration (Gilmore et al., 1998; Molnar et al., 1998; Pinto Lord et al., 1982). Although chronic ethanol exposure from E8 is known to disrupt cortical column structure (Gressens et al., 1992), it is likely that ethanol-induced disruption of preplate splitting at E13-E15 could trigger neuroanatomical and therefore functional deficits. For example, a single dose of ethanol during the period of preplate splitting in rat cortex leads to ectopic pyramidal neurons in the molecular and external granular layers, as well as a loss of layer 4 neurons (Ferreira et al., 2004). In contrast, a single incident of ethanol exposure at later developmental time points has more modest effects on cellular morphology (Granato and Van Pelt, 2003). Minimally a sustained alteration of early dendrite formation in L6 neurons is likely to impact their signaling interactions and synapse formation with Layer 1 (presynaptic) neurons. Altered dendritic morphology might then alter the number or effectiveness of synapses that are generated during later development, and the subsequent ability of the dendritic arbor to integrate synaptic signals. In this sense, even modest prenatal exposure to ethanol could negatively and persistently impact development and function in the postnatal period.

Supplementary Material

Refer to Web version on PubMed Central for supplementary material.

Acknowledgments

Funding

This work was supported by the Developmental Exposure to Alcohol Research Center (DEARC) NIAAA (P50AA017823-5985) to ECO.

The authors thank the following: Judson Belmont for technical support. Candida Ustine for developing the MATLAB script, Dr. David Cameron for comment and edits on the manuscript, Dr. Robert Quinn and the staff in the Department of Laboratory Animal Resources for animal care.

References

Aronne MP, Guadagnoli T, Fontanet P, Evrard SG, Brusco A. Effects of prenatal ethanol exposure on rat brain radial glia and neuroblast migration. Exp Neurol. 2011; 229:364–371. [PubMed: 21414313]

Behar O, Golden JA, Mashimo H, Schoen FJ, Fishman MC. Semaphorin III is needed for normal patterning and growth of nerves, bones and heart. Nature. 1996; 383:525–528. [PubMed: 8849723]

Camarillo C, Miranda RC. Ethanol exposure during neurogenesis induces persistent effects on neural maturation: evidence from an ex vivo model of fetal cerebral cortical neuroepithelial progenitor maturation. Gene Expr. 2008; 14:159–171. [PubMed: 18590052]

Chen WJ, McAlhany RE Jr, West JR. 4-Methylpyrazole, an alcohol dehydrogenase inhibitor, exacerbates alcohol-induced microencephaly during the brain growth spurt. Alcohol. 1995; 12:351–355. [PubMed: 7546332]

de Anda FC, Meletis K, Ge X, Rei D, Tsai LH. Centrosome motility is essential for initial axon formation in the neocortex. J Neurosci. 2010; 30:10391–10406. [PubMed: 20685982]

Dotti CG, Banker GA. Experimentally induced alteration in the polarity of developing neurons. Nature. 1987; 330:254–256. [PubMed: 3313064]

Dotti CG, Sullivan CA, Banker GA. The establishment of polarity by hippocampal neurons in culture. J Neurosci. 1988; 8:1454–1468. [PubMed: 3282038]

Ferreira TA, Ferreira NR, Morais JOM, Penha-Silva N. Effects of acute prenatal exposure to ethanol on the postnatal morphology of the prefrontal cortex in Wistar rats. Braz J Morphol Sci. 2004; 21:99–103.

Gilmore EC, Ohshima T, Goffinet AM, Kulkarni AB, Herrup K. Cyclin-dependent kinase 5-deficient mice demonstrate novel developmental arrest in cerebral cortex. J Neurosci. 1998; 18:6370–6377. [PubMed: 9698328]

Goodlett CR, Horn KH. Mechanisms of alcohol-induced damage to the developing nervous system. Alcohol Res Health. 2001; 25:175–184. [PubMed: 11810955]

Granato A, Di Rocco F, Zumbo A, Toesca A, Giannetti S. Organization of cortico-cortical associative projections in rats exposed to ethanol during early postnatal life. Brain Res Bull. 2003; 60:339–344. [PubMed: 12781322]

Granato A, Palmer LM, De Giorgio A, Tavian D, Larkum ME. Early exposure to alcohol leads to permanent impairment of dendritic excitability in neocortical pyramidal neurons. J Neurosci. 2012; 32:1377–1382. [PubMed: 22279222]

Granato A, Van Pelt J. Effects of early ethanol exposure on dendrite growth of cortical pyramidal neurons: inferences from a computational model. Brain Res Dev Brain Res. 2003; 142:223–227.

Greenberg DA. Linking acquired neurodevelopmental disorders to defects in cell adhesion. Proc Natl Acad Sci USA. 2003; 100:8043–8044. [PubMed: 12835424]

Gressens P, Lammens M, Picard JJ, Evrard P. Ethanol-induced disturbances of gliogenesis and neuronogenesis in the developing murine brain: an in vitro and in vivo immunohistochemical and ultrastructural study. Alcohol Alcohol. 1992; 27:219–226. [PubMed: 1449557]

Hamby-Mason R, Chen JJ, Schenker S, Perez A, Henderson GI. Catalase mediates acetaldehyde formation from ethanol in fetal and neonatal rat brain. Alcohol Clin Exp Res. 1997; 21:1063–1072. [PubMed: 9309319]

Hamilton GF, Whitcher LT, Klintsova AY. Postnatal binge-like alcohol exposure decreases dendritic complexity while increasing the density of mature spines in mPFC Layer II/III pyramidal neurons. Synapse. 2010; 64:127–135. [PubMed: 19771589]

Hatanaka Y, Yamauchi K. Excitatory Cortical Neurons with Multipolar Shape Establish Neuronal Polarity by Forming a Tangentially Oriented Axon in the Intermediate Zone. Cereb Cortex. 2012 Epub ahead of press.

Horton AC, Racz B, Monson EE, Lin AL, Weinberg RJ, Ehlers MD. Polarized secretory trafficking directs cargo for asymmetric dendrite growth and morphogenesis. Neuron. 2005; 48:757–771. [PubMed: 16337914]

Jones KL, Smith DW. Recognition of the fetal alcohol syndrome in early infancy. Lancet. 1973; 302:999–1001. [PubMed: 4127281]

Kodani A, Sutterlin C. A new function for an old organelle: microtubule nucleation at the Golgi apparatus. EMBO. 2009; 28:995–996.

Komatsu S, Sakata-Haga H, Sawada K, Hisano S, Fukui Y. Prenatal exposure to ethanol induces leptomeningeal heterotopia in the cerebral cortex of the rat fetus. Acta neuropathol. 2001; 101:22–26. [PubMed: 11194937]

Lawrence RC, Otero NK, Kelly SJ. Selective effects of perinatal ethanol exposure in medial prefrontal cortex and nucleus accumbens. Neurotoxicol Teratol. 2012; 34:128–135. [PubMed: 21871563]

Lindsley TA, Kerlin AM, Rising LJ. Time-lapse analysis of ethanol's effects on axon growth in vitro. Brain Res Dev Brain Res. 2003; 147:191–199.

Livy DJ, Elberger AJ. Alcohol exposure during the first two trimesters-equivalent alters the development of corpus callosum projection neurons in the rat. Alcohol. 2008; 42:285–293. [PubMed: 18468834]

Longair MH, Baker DA, Armstrong JD. Simple Neurite Tracer: open source software for reconstruction, visualization and analysis of neuronal processes. Bioinformatics. 2011; 27:2453–2454. [PubMed: 21727141]

Luo Y, Shepherd I, Li J, Renzi MJ, Chang S, Raper JA. A family of molecules related to collapsin in the embryonic chick nervous system. Neuron. 1995; 14:1131–1140. [PubMed: 7605628]

Marin MP, Esteban-Pretel G, Ponsoda X, Romero AM, Ballestin R, Lopez C, Megias L, Timoneda J, Molowny A, Canales JJ, et al. Endocytosis in cultured neurons is altered by chronic alcohol exposure. Toxicol Sci. 2010; 115:202–213. [PubMed: 20133374]

Marin-Padilla M. Dual origin of the mammalian neocortex and evolution of the cortical plate. Anat Embryol (Berl). 1978; 152:109–126. [PubMed: 637312]

Marinari UM, Pronzato MA, Pizzorno R, Cottalasso D, Maloberti G, Domenicotti C, Gazzo P, Nanni G. Acetaldehyde-induced impairment of protein glycosylation in liver Golgi apparatus. Biochem Mol Biol Int. 1993; 29:1131–1138. [PubMed: 8330019]

Matsuda T, Cepko CL. Electroporation and RNA interference in the rodent retina in vivo and in vitro. Proc Natl Acad Sci USA. 2004; 101:16–22. [PubMed: 14603031]

Matsuki T, Matthews RT, Cooper JA, van der Brug MP, Cookson MR, Hardy JA, Olson EC, Howell BW. Reelin and stk25 have opposing roles in neuronal polarization and dendritic Golgi deployment. Cell. 2010; 143:826–836. [PubMed: 21111240]

Megias L, Guerri C, Fornas E, Azorin I, Bendala E, Sancho-Tello M, Duran JM, Tomas M, Gomez-Lechon MJ, Renau-Piqueras J. Endocytosis and transcytosis in growing astrocytes in primary culture. Possible implications in neural development. Int J Devel Biol. 2000; 44:209–221. [PubMed: 10794079]

Molnar Z, Adams R, Goffinet AM, Blakemore C. The role of the first postmitotic cortical cells in the development of thalamocortical innervation in the reeler mouse. J Neurosci. 1998; 18:5746–5765. [PubMed: 9671664]

Nakamura N, Rabouille C, Watson R, Nilsson T, Hui N, Slusarewicz P, Kreis TE, Warren G. Characterization of a cis-Golgi matrix protein, GM130. J Cell Biol. 1995; 131:1715–1726. [PubMed: 8557739]

Nichols AJ, Olson EC. Reelin promotes neuronal orientation and dendritogenesis during preplate splitting. Cereb Cortex. 2010; 20:2213–2223. [PubMed: 20064940]

O'Dell RS, Ustine CM, Cameron DA, Lawless SM, Williams RM, Zipfel WR, Olson EC. Layer 6 cortical neurons require Reelin-Dab1 signaling for cellular orientation, Golgi deployment, and directed neurite growth into the marginal zone. Neural Dev. 2012 Epub ahead of print.

Olson EC, Kim S, Walsh CA. Impaired neuronal positioning and dendritogenesis in the neocortex after cell-autonomous Dab1 suppression. J Neurosci. 2006; 26:1767–1775. [PubMed: 16467525]

Pinto Lord MC, Evrard P, Caviness VS Jr. Obstructed neuronal migration along radial glial fibers in the neocortex of the reeler mouse: a Golgi-EM analysis. Brain Res. 1982; 256:379–393. [PubMed: 7127145]

Qu W, Wu D. [Effects of alcohol and metabolite acetaldehyde on the proliferation of astroglial cells of fetal brain]. Wei sheng yan jiu. J Hygiene Res. 1999; 28:206–207.

Romero AM, Esteban-Pretel G, Marin MP, Ponsoda X, Ballestin R, Canales JJ, Renau-Piqueras J. Chronic ethanol exposure alters the levels, assembly, and cellular organization of the actin cytoskeleton and microtubules in hippocampal neurons in primary culture. Toxicol Sci. 2010; 118:602–612. [PubMed: 20829428]

Sepulveda B, Carcea I, Zhao B, Salton SR, Benson DL. L1 cell adhesion molecule promotes resistance to alcohol-induced silencing of growth cone responses to guidance cues. Neuroscience. 2011; 180:30–40. [PubMed: 21335065]

Serafini T, Kennedy TE, Galko MJ, Mirzayan C, Jessell TM, Tessier-Lavigne M. The netrins define a family of axon outgrowth-promoting proteins homologous to C. elegans UNC-6. Cell. 1994; 78:409–424. [PubMed: 8062384]

Shelly M, Cancedda L, Lim BK, Popescu AT, Cheng PL, Gao H, Poo MM. Semaphorin3A Regulates Neuronal Polarization by Suppressing Axon Formation and Promoting Dendrite Growth. Neuron. 2011; 71:433–446. [PubMed: 21835341]

Shelly M, Poo MM. Role of LKB1-SAD/MARK pathway in neuronal polarization. Dev Neurobiol. 2011; 71:508–527. [PubMed: 21416623]

Steup A, Lohrum M, Hamscho N, Savaskan NE, Ninnemann O, Nitsch R, Fujisawa H, Puschel AW, Skutella T. Sema3C and netrin-1 differentially affect axon growth in the hippocampal formation. Mol Cell Neurosci. 2000; 15:141–155. [PubMed: 10673323]

Tabata H, Nakajima K. Multipolar migration: the third mode of radial neuronal migration in the developing cerebral cortex. J Neurosci. 2003; 23:9996–10001. [PubMed: 14602813]

Takahashi T, Nowakowski RS, Caviness VS Jr. The cell cycle of the pseudostratified ventricular epithelium of the embryonic murine cerebral wall. J Neurosci. 1995; 15:6046–6057. [PubMed: 7666188]

Tanabe K, Kani S, Shimizu T, Bae YK, Abe T, Hibi M. Atypical protein kinase C regulates primary dendrite specification of cerebellar Purkinje cells by localizing Golgi apparatus. J Neurosci. 2010; 30:16983–16992. [PubMed: 21159968]

Tomas M, Fornas E, Megias L, Duran JM, Portoles M, Guerri C, Egea G, Renau-Piqueras J. Ethanol impairs monosaccharide uptake and glycosylation in cultured rat astrocytes. J Neurochem. 2002; 83:601–612. [PubMed: 12390522]

Tomas M, Marin P, Megias L, Egea G, Renau-Piqueras J. Ethanol perturbs the secretory pathway in astrocytes. Neurobiology of disease. 2005; 20:773–784. [PubMed: 15953732]

Whitcher LT, Klintsova AY. Postnatal binge-like alcohol exposure reduces spine density without affecting dendritic morphology in rat mPFC. Synapse. 2008; 62:566–573. [PubMed: 18512209]

Yanni PA, Rising LJ, Ingraham CA, Lindsley TA. Astrocyte-derived factors modulate the inhibitory effect of ethanol on dendritic development. Glia. 2002; 38:292–302. [PubMed: 12007142]

Ye B, Zhang Y, Song W, Younger SH, Jan LY, Jan YN. Growing dendrites and axons differ in their reliance on the secretory pathway. Cell. 2007; 130:717–729. [PubMed: 17719548]

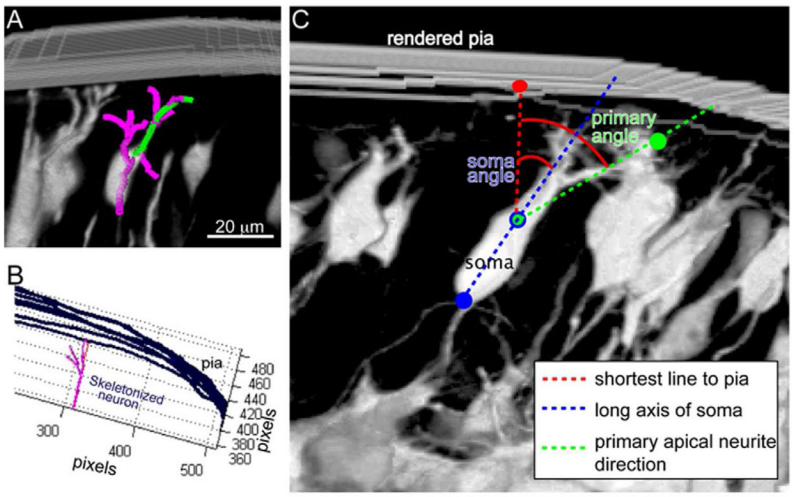

Figure 1. Morphological Analyses

(A) Complete 3-D neuronal reconstructions were performed by importing confocal z-stacks into FIJI and using Simple Neurite Tracer to trace the primary apical (green) and complete apical neurite arbor (pink). Neurite length and branching values were then obtained from these 3-D reconstructions (B) To determine orientation angles of the primary dendrite and soma, the skeletonized neuron (pink) and contour lines representing the pial surface (blue) were imported into a custom MATLAB script. (C) The line in 3-D space connecting the neuronal soma to the closest point on the pial surface was identified (red) and the angles that the primary apical neurite (green) and the long axis of the soma (blue) make with respect to that connecting line was calculated. Scale bar, 20 μm.

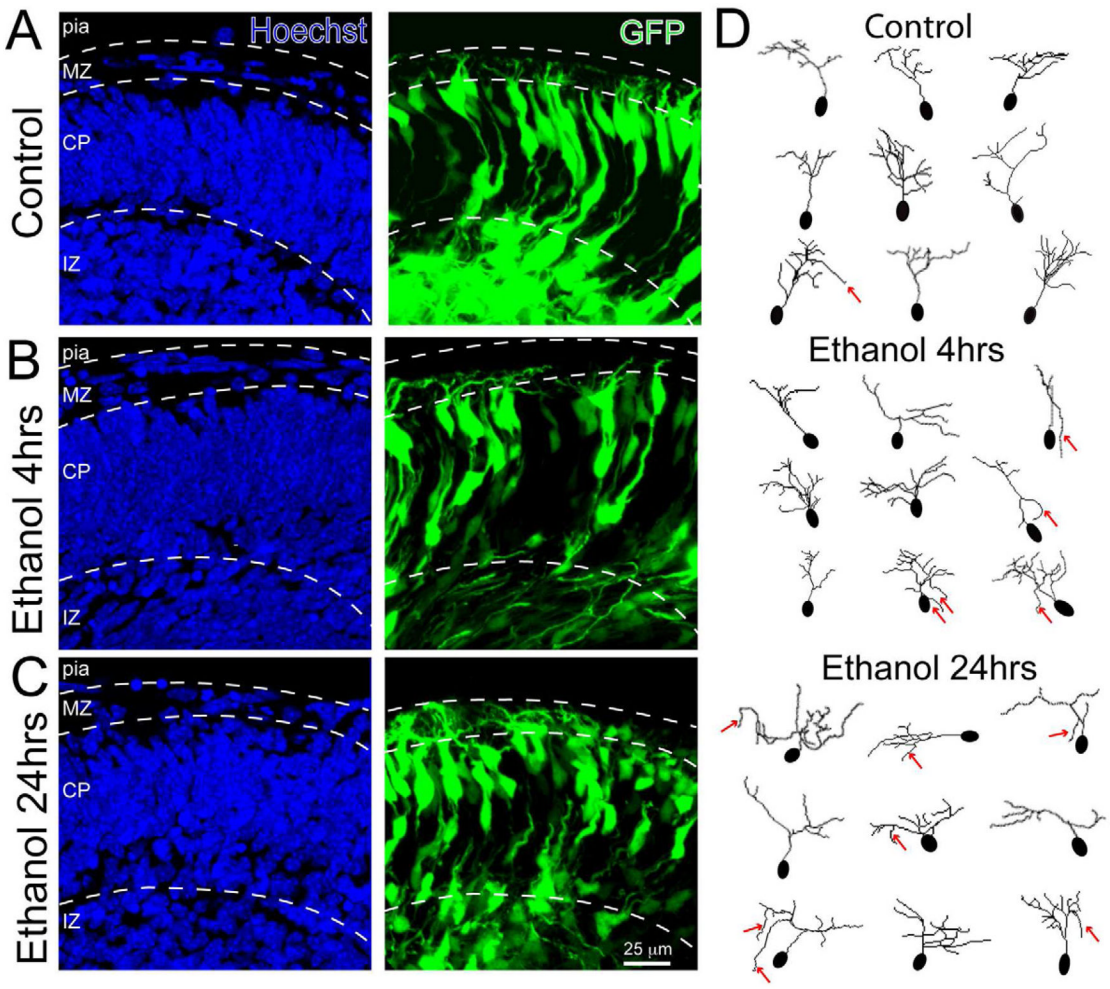

Figure 2. L6 cortical neuron response to 4 and 24 hrs of ethanol exposure

Confocal images of explant sections containing (A) control L6 neurons, (B) L6 neurons after 4 hrs of ethanol exposure, and (C) L6 neurons after 24 hrs of ethanol exposure. Disruption of somal and primary apical neurite orientation is apparent after 24 hrs of ethanol treatment. The neurons are labeled with GFP (green) and the sections were counterstained with Hoechst nuclear dye (blue) to reveal overall cortical histology. (D) 3-D neuronal traces obtained with Simple Neurite Tracer were flattened to illustrate the differences in neuronal morphologies between treatment conditions. The red arrows indicate examples of aberrant neurites growing away from the pial surface. Scale bar, 25 μm; MZ, marginal zone; CP, cortical plate; IZ, intermediate zone.

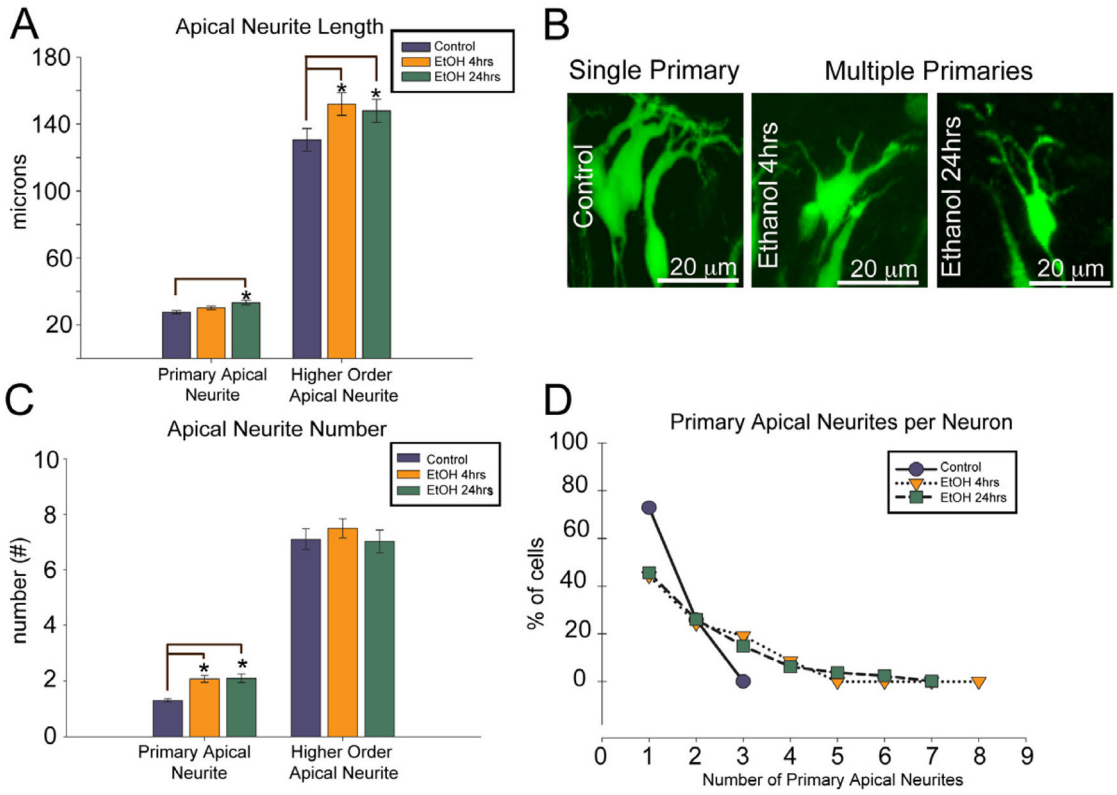

Figure 3. Apical neurite growth and branching after ethanol exposure

(A) Quantified main primary apical neurite (longest primary extending from the cell body) and higher order apical neurite length after 4 and 24 hrs ethanol exposure (mean ± SEM). (B) Examples of neurons with single and multiple primary apical neurite (arrows). (C) Quantification of the average number of primary apical neurites *per* neuron, and the higher order apical neurite number *per* neuron, after 4 and 24 hr ethanol exposure (mean ± SEM) (D) Distribution of neurons based on the number of primary neurites. n=85, 114, and 81 for control, 4 and 24 hr ethanol, respectively. The single asterisk (*) denotes $p < 0.05$, ANOVA across treatments followed by a Dunn post-hoc test. Scale bar, 20 µm.

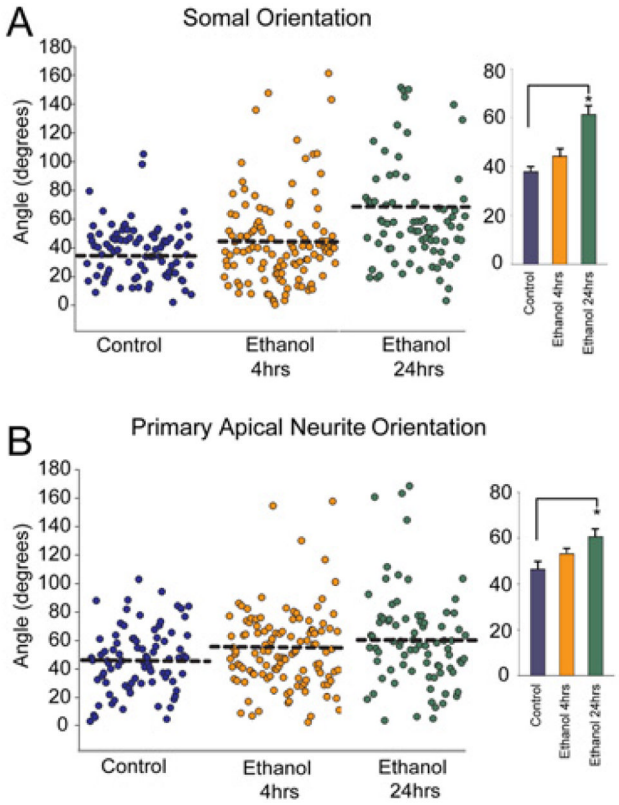

Figure 4. Somal and primary dendrite orientation after ethanol exposure

(A) Somal and (B) Apical neurite orientation angles calculated from 3-D reconstructions of individual neurons after 4 and 24 hr ethanol exposure. Each plot point represents the angle of an individual neuron. The bar graphs indicate the orientation angle (mean ± SEM) within each treatment condition. 24 hrs of ethanol exposure causes a significant change in both somal and apical neurite orientation angles. n=85, 114, and 81 for control, 4 hr, and 24 hr ethanol, respectively. The single asterisk (*) denotes $p < 0.05$, ANOVA across treatments followed by a Dunn post-hoc test.

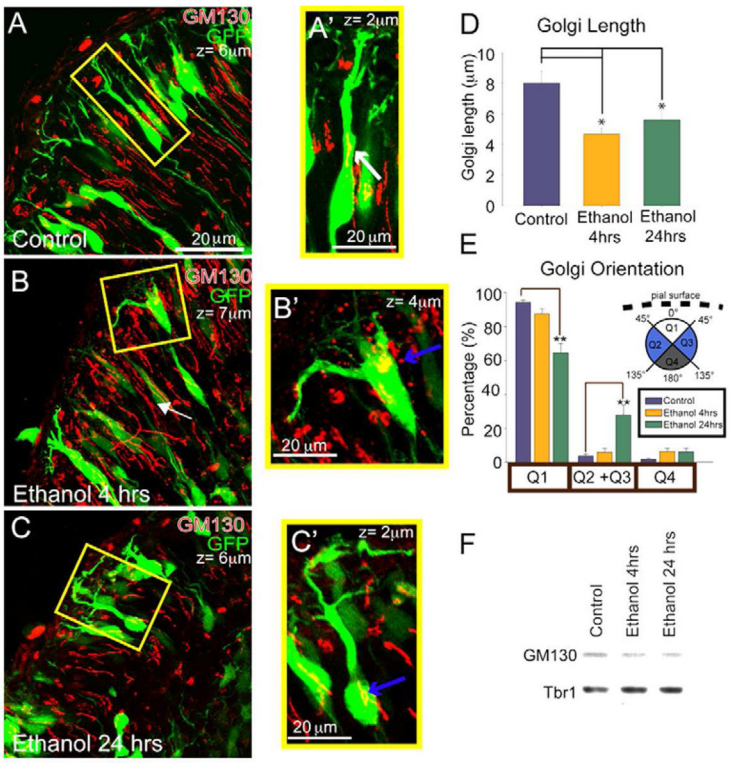

Figure 5. Golgi apparatus compaction and repositioning after ethanol exposure

Immunolabeling with the cis-Golgi marker GM130 (red) reveals elongated Golgi (white arrows) within the apical neurite of GFP+ neurons in A, A′) control explants and compacted Golgi (blue arrows) within GFP+ neurons in B, B′) 4 hr and C, C′) 24 hr ethanol exposed explants. The z-stack depths in μm are denoted in the upper right of each image and the enlarged images (A′-C′) are smaller in z-depth to capture only those Golgi contained in the identified GFP+ cell. D) Proximal-to-distal Golgi length measurements (mean ± SEM). The single asterisk (*) denotes $p < 0.05$, ANOVA across treatments followed by a Dunn post-hoc test. E) Localization of Golgi in neuronal soma by quadrants (Q1–4). 24 hrs of ethanol exposure causes a significant relocalization of the Golgi into lateral quadrants (Q2+Q4) from the apical quadrant (Q1). n=41, 38, and 41 for control, 4 hr, and 24 hr ethanol, respectively. (F) Immunoblot of GM130 protein in lysates of whole hemispheric cortical explants following 4 and 24 hr ethanol exposure. The transcription factor Tbr1 was used as a loading control. The double asterisk (**) denotes $p < 0.01$, ANOVA across treatments followed by Fishers LSD between conditions and quadrants. Scale bar, 20μm.

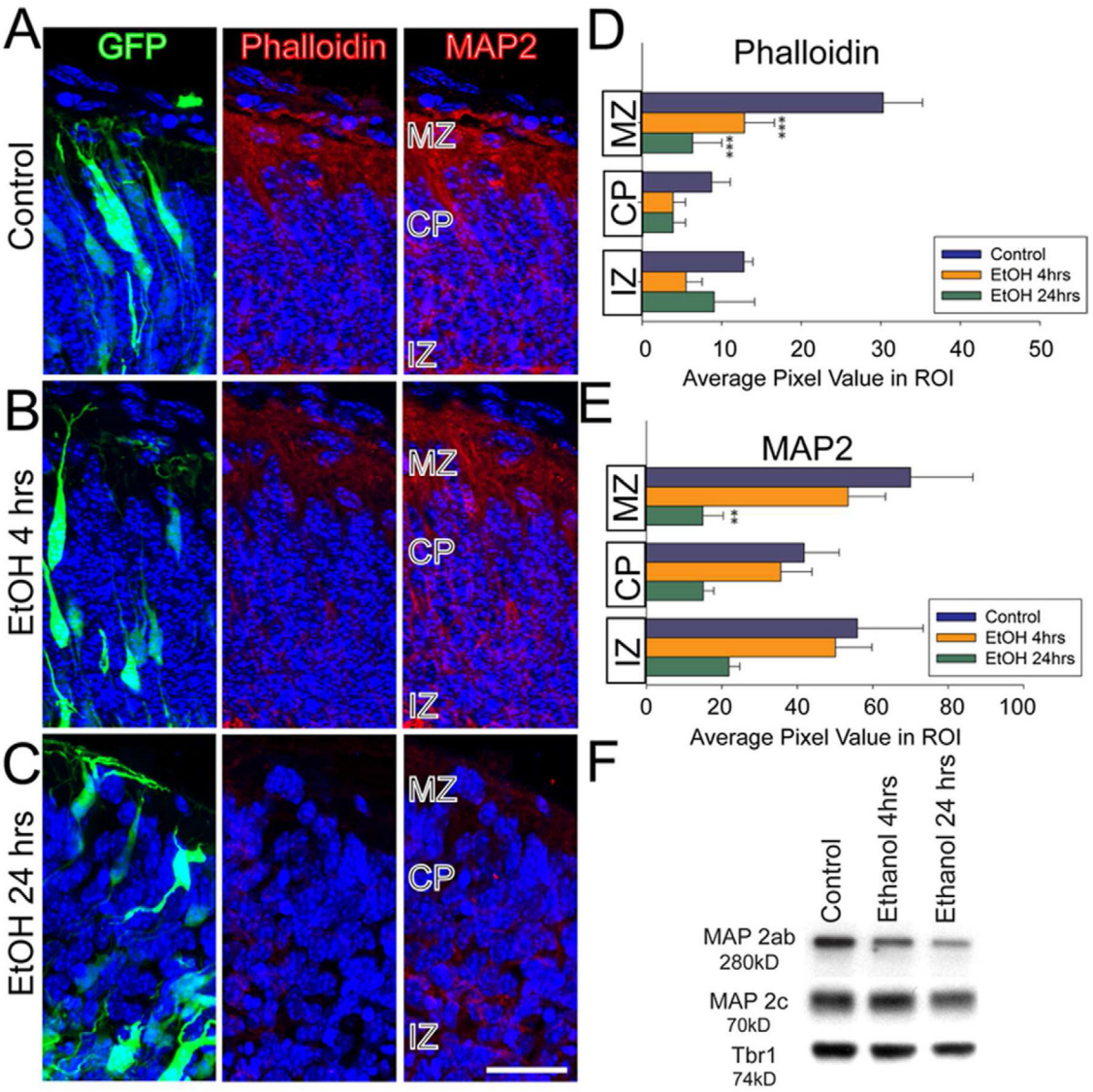

Figure 6. Reduction of F-actin and MAP2 content after ethanol exposure

(A) The first column shows GFP-expressing (green) neuronal morphology and Hoechst nuclear dye (blue) to provide overall cortical histology. The second column is the corresponding AlexaFluor-Phalloidin (F-actin: red) labeling of the same explant sections, illustrating a reduction in label signal specific to the MZ after (B) 4 hrs and (C) 24 hrs ethanol exposure. The third column demonstrates a similar decrease in MAP2 immunosignal (red) that is restricted to the MZ after 24 hr exposure (C). (D, E) Quantified MAP2 and Phalloidin signal. The summed pixel values for a defined ROI in each cortical zone in each condition are reported and compared. n=4, 4, and 3 for control, 4 hr, and 24 hr ethanol, respectively. (F) MAP2 immunoblotting on whole hemisphere cortical explants. MAP2ab appear as a single 280kD band during early cortical development whereas the immature form, MAP2c is 70kD. Ethanol treatment decreased mature MAP2 content without significantly affecting immature MAP expression. The Tbr1 band provides a protein loading control. A 3 treatment × 3 ROI mixed model ANOVA was performed followed by post-hoc Fisher LSD. $*p < 0.05$, $**p < 0.01$, $***p < 0.001$. Scale bar, 20 μm.